

RESEARCH ARTICLE | AUGUST 04 2022

Zero-cost corrections to influence functional coefficients from bath response functions

Amartya Bose  



J. Chem. Phys. 157, 054107 (2022)
<https://doi.org/10.1063/5.0101396>



Articles You May Be Interested In

A multisite decomposition of the tensor network path integrals

J. Chem. Phys. (January 2022)

Topological aspects of system-bath Hamiltonians and a vector model for multisite systems coupled to local, correlated, or common baths

J. Chem. Phys. (April 2023)

Collective bath coordinate mapping of “hierarchy” in hierarchical equations of motion

J. Chem. Phys. (March 2022)



The Journal of Chemical Physics
**Special Topics Open
for Submissions**

[Learn More](#)

 AIP
Publishing

Zero-cost corrections to influence functional coefficients from bath response functions

Cite as: J. Chem. Phys. 157, 054107 (2022); doi: 10.1063/5.0101396

Submitted: 31 May 2022 • Accepted: 10 July 2022 •

Published Online: 4 August 2022



View Online



Export Citation



CrossMark

Amartya Bose^{a)} 

AFFILIATIONS

Department of Chemistry, Princeton University, Princeton, New Jersey 08544, USA

^{a)}Author to whom correspondence should be addressed: amartyab@princeton.edu and amartya.bose@gmail.com

ABSTRACT

Recent work has shown that it is possible to circumvent the calculation of the spectral density and directly generate the coefficients of the discretized influence functionals using data from classical trajectory simulations. However, the accuracy of this procedure depends on the validity of the high temperature approximation. In this work, an alternative derivation based on the Kubo formalism is provided. This enables the calculation of additional correction terms that increases the range of applicability of the procedure to lower temperatures. Because it is based on the Kubo-transformed correlation function, this approach allows the direct use of correlation functions obtained from methods such as ring-polymer molecular dynamics and centroid molecular dynamics in determining the influence functional coefficients for subsequent system-solvent simulations. The accuracy of the original procedure and the corrected procedure is investigated across a range of parameters. It is interesting that the correction term comes at zero additional cost. Furthermore, it is possible to improve upon the correction using zero-cost physical intuition and heuristics making the method even more accurate.

Published under an exclusive license by AIP Publishing. <https://doi.org/10.1063/5.0101396>

I. INTRODUCTION

Simulation of quantum dynamics in the condensed phase is a challenging problem. Classical mechanics can often be a very approachable approach to such simulations. These classical calculations miss out on corrections coming from quantum dispersion and zero-point energy effects. Much work has been done to incorporate quantum effects in classical trajectories ranging from full semiclassical dynamics^{1–3} to single classical trajectory-based approaches, such as the Wigner approach,^{4,5} centroid molecular dynamics (CMD),^{6,7} and ring-polymer molecular dynamics (RPMD).⁸ However, for problems where the quantum nature of the dynamics is inevitable, these classical trajectory-based approaches are not useful. Often in such cases, a system-solvent decomposition can be performed limiting the quantum nature of the dynamics to a low-dimensional subspace. Typically, reduced density matrix approaches related to the hierarchical equations of motion (HEOM)⁹ and quasi-adiabatic propagator path integral (QuAPI)^{10,11} are used for such problems.

Recently, tensor network approaches have been used in conjunction with both HEOM^{12–14} and QuAPI.^{15–17} Based on the tensor network representation of path integral using the Feynman–Vernon

influence functional,¹⁸ one can develop a multi-site method that is capable of simulating extended quantum systems.¹⁹ This new multi-site tensor network path integral has been used to study the dynamics and absorption spectra of the B850 ring²⁰ and diffusive quantum transport in XXZ spin-chains coupled with phonons.²¹ The presence of the solvent makes the time propagation of the system non-Markovian. In the path integral framework, this non-Markovian memory is expressed as two-point interactions characterized by the separation between them. These interaction coefficients are related to integrals of the bath response function and have historically been expressed as integrals over the spectral density. While this is convenient for model studies with analytical spectral densities, it necessitates high quality molecular dynamics (MD) simulations for estimating the spectral density when the solvent is atomistically described. The presence of numerical noise in these molecular dynamics simulations along with the requirement to simulate up to long times to reach equilibrium complicate the calculation of these spectral densities.

Allen *et al.*²² have proposed a technique to directly use the energy gap autocorrelation function to estimate the influence functional coefficients required for a path integral simulation and avoid the computation of the spectral density. While this classical

approximation (CA) method is extremely simple, its basic assumptions limit its applicability only to high temperatures. This stems from the simultaneous identification of the classical correlation function and its derivative with the real and imaginary parts of the quantum correlation function, respectively. It is quite well-understood that the quantum dispersion and zero-point effects would affect the real part significantly in all but the highest temperatures. The basic goal of this paper is to derive a similarly computationally efficient method of obtaining the discretized influence functional coefficients from the bath response function but with better accuracy at lower temperatures.

Before going further, it would be prudent to note that this discussion is based on the presumption that the potential energy surface describing the dynamics is *ab initio*. Although *ab initio* molecular dynamics (AIMD) is becoming increasingly approachable for large systems using neural network fits of the forces and energies from density functional theory,^{23,24} classical force-fields such as Chemistry at Harvard Molecular Mechanics (CHARMM)²⁵ still remain extremely popular. These classical force fields are generally designed with the goal of including nuclear quantum effects at particular thermodynamic conditions. When the scheme is successful, the solvent described by such classical force fields can approximately account for nuclear quantum effects through classical mechanics. In such cases, the simultaneous identification of the real and imaginary part of the quantum correlation function with the classical correlation function and its derivative, respectively, in CA is correct. The rest of this paper assumes some sort of an *ab initio* description that is not parameterized to account for the nuclear quantum effects of the solvent.

In this paper, we propose an approach to deriving the discretized influence functional coefficients directly in terms of the Kubo-transformed bath response function. The Kubo-transform of the bath response function is given by

$$\alpha_{\text{Kubo}}(t) = \frac{1}{\beta Q} \int_0^\beta d\lambda \text{Tr} [e^{-(\beta-\lambda)\hat{H}_{\text{sol}}} \hat{f} e^{-\lambda\hat{H}_{\text{sol}}} \hat{f}(t)]. \quad (1)$$

The Kubo correlation function is commonly simulated by methods for simulating approximate quantum dynamics, such as centroid molecular dynamics (CMD)^{6,7} and ring-polymer molecular dynamics (RPMD).⁸ While there are many ways of expressing the quantum correlation function, the Kubo formulation is widely known to be the most similar to the classical correlation function. The explicit formulation of the η -coefficient in terms of the Kubo correlation function presented here creates a clear link between methods such as CMD and RPMD and Feynman–Vernon influence functional-based path integral.

This new derivation not only provides an alternative to the CA approach²² but additionally gives a full series expansion. Consequently, it becomes easy to improve the results by incorporating the leading order corrections while retaining all the numerical advantages of CA. We show that the most important first-order correction term can be analytically simplified and written in terms of the bath response function. The idea behind the incorporation of these higher order terms is to correct for the discrepancy brought in by assuming that the classical correlation function does an adequate job of representing the real part of the quantum correlation function. These higher order terms are dependent on time-derivatives

of the bath response functions. Numerical derivatives are extremely sensitive to noise present in the data. Therefore, we have expressed the second-order correction in terms of a different correlation function. Every extra order of correction either requires a calculation of completely different correlation functions or numerical derivatives. This makes it impractical to go to very high orders. We have further improved the first-order correction through physical arguments and heuristics. The errors in CA and the corrected methods are evaluated with respect to the η -coefficients and the dynamics. The most attractive aspect of the first-order and the heuristic corrections is that they can be done completely free of any additional cost, retaining the dependence only on the energy-gap correlation function.

The methods are derived in Sec. II, and a variety of numerical tests and illustrations are shown in Sec. III. In addition, an approach to rigorously obtain the next correction term is derived in the Appendix. We end this paper in Sec. IV with some conclusions and observations regarding these efforts to use the classical or semiclassical correlation function directly in the generation of the discretized influence functional coefficients.

II. METHOD

Consider a quantum system coupled with a dissipative solvent,

$$\hat{H} = \hat{H}_0 + \hat{H}_{\text{sol}}, \quad (2)$$

where \hat{H}_0 is the Hamiltonian describing the quantum system and \hat{H}_{sol} describes the dissipative solvent. If the system is a two-level system, $\hat{H}_0 = \epsilon \hat{\sigma}_z - \hbar \Omega \hat{\sigma}_x$, where $\hat{\sigma}_{x,y,z}$ are the Pauli spin matrices.

The thermal dissipative solvent in many cases is atomistically described. If the fully atomistic description needs to be considered, one can use various mixed quantum–classical methods such as the quantum–classical path integral method^{26,27} for simulation. However, generally, it is possible to map the essentially anharmonic solvent onto a harmonic bath under the Gaussian response theory. In such a case, the harmonic bath and its interactions with the system are characterized by a spectral density,

$$J(\omega) = \frac{\pi}{2} \sum_j \frac{c_j^2}{m_j \omega_j} \delta(\omega - \omega_j), \quad (3)$$

where ω_j and c_j are the frequency and the coupling of the j th harmonic oscillator to the system, respectively. Under the harmonic bath, the Hamiltonian of the environment is given by

$$\hat{H}_{\text{sol}} = \sum_j \frac{\hat{p}_j^2}{2m_j} + \frac{1}{2} m \omega_j^2 \left(\hat{x}_j - \frac{c_j \hat{s}}{m_j \omega_j^2} \right)^2, \quad (4)$$

where \hat{s} is the operator that couples the system with the solvent.

The spectral density, for this harmonic mapping, is obtained from the solvent energy gap correlation function also called the bath response function. It is related to the spectrum corresponding to the bath response function as follows:

$$\alpha(\omega) = \frac{2J(\omega)}{1 - \exp(-\hbar\omega\beta)}. \quad (5)$$

Consequently, the bath response function is given by

$$\alpha(t) = \frac{1}{\pi} \int_0^\infty d\omega J(\omega) \left(\coth\left(\frac{\hbar\omega\beta}{2}\right) \cos(\omega t) - i \sin(\omega t) \right). \quad (6)$$

If the initial condition is specified as a direct product of the system reduced density matrix and the bath thermal density, then the system reduced density matrix after N time-steps of length Δt can be represented as a path integral,

$$\begin{aligned} \langle s_N^+ | \rho(N\Delta t) | s_N^- \rangle &= \sum_{s_0^+} \sum_{s_1^+} \dots \sum_{s_{N-1}^+} \langle s_N^+ | \hat{U} | s_{N-1}^+ \rangle \langle s_{N-1}^+ | \hat{U} | s_{N-2}^+ \rangle \\ &\times \dots \langle s_1^+ | \hat{U} | s_0^+ \rangle \langle s_0^+ | \rho(0) | s_0^- \rangle \langle s_0^- | \hat{U}^\dagger | s_1^- \rangle \\ &\times \dots \langle s_{N-1}^- | \hat{U}^\dagger | s_N^- \rangle F[\{s_j^\pm\}], \end{aligned} \quad (7)$$

where

$$F[\{s_j^\pm\}] = \exp\left(-\frac{1}{\hbar} \sum_{k=0}^N (s_k^+ - s_k^-) \sum_{k'=0}^k (\eta_{kk'} s_{k'}^+ - \eta_{kk'}^* s_{k'}^-)\right), \quad (8)$$

where \hat{U} is the short time system propagator and s_j^\pm is the forward-backward state of the system at the j th time point. The Feynman–Vernon influence function¹⁸ is denoted by $F[\{s_j^\pm\}]$, which is dependent upon the history of the path. This influence functional can be described in terms of certain η -coefficients^{10,11} and can be expressed as double integrals of $\alpha(t)$. The most general form is given as

$$\eta_{kk'} = \int_{(k-\frac{1}{2})\Delta t}^{(k+\frac{1}{2})\Delta t} dt' \int_{(k'-\frac{1}{2})\Delta t}^{(k'+\frac{1}{2})\Delta t} dt'' \alpha(t' - t''). \quad (9)$$

The spectral density and the correlation functions required here are quantum mechanical. However, due to the large dimensionality of the solvent, one has to resort to classical trajectory-based approximations to the quantum dynamics. The most popular such approaches are CMD⁷ and RPMD.⁸ These approaches estimate the Kubo transform of a given correlation function,

$$\alpha_{\text{Kubo}}(t) = \frac{1}{\beta Q} \int_0^\beta d\lambda \text{Tr} \left[e^{-(\beta-\lambda)\hat{H}_{\text{sol}}} \hat{f} e^{-\lambda\hat{H}_{\text{sol}}} \hat{f}(t) \right]. \quad (10)$$

The main allure behind the Kubo-transformed correlation function is that it has many similarities in structure with the classical correlation function. Thus, departing from the classical approximation (CA),²² we assume that if only a classical correlation function is available, it is more prudent to use it as an approximation to the Kubo-transformed correlation function. (The rest of this section deals only with $\alpha_{\text{Kubo}}(t)$ and its derivatives.)

It is well-known that the Kubo-transformed correlation function has identical information to the standard correlation function. In particular, the standard spectrum is related to the Kubo spectrum by

$$\alpha(\omega) = \frac{\hbar\omega\beta}{1 - \exp(-\hbar\omega\beta)} \alpha_{\text{Kubo}}(\omega). \quad (11)$$

Because the Kubo correlation function is even and consequently, the Kubo spectrum is symmetric, one can relate the spectral density to the Kubo spectrum,

$$J(\omega) = \frac{\hbar\omega\beta}{2} \alpha_{\text{Kubo}}(\omega). \quad (12)$$

It is possible to use the spectral density from the approximate quantum calculations in our estimation of the η -coefficients.

However, generating accurate, noise-free quantum correlation functions for the Fourier transform involved in the calculation of the spectral density can be challenging for large systems. It has been shown that expressing the η -coefficients directly in terms of the correlation function can make the approach numerically robust.²²

We can relate the bath response function to the Kubo correlation function estimated by substituting Eq. (12) in Eq. (6), expanding the coth term to a series and doing the integrals,

$$\begin{aligned} \alpha(t) &= \alpha_{\text{Kubo}}(t) + \frac{i\hbar\beta}{2} \dot{\alpha}_{\text{Kubo}}(t) + \frac{1}{3} \left(\frac{i\hbar\beta}{2} \right)^2 \ddot{\alpha}_{\text{Kubo}}(t) \\ &- \frac{1}{45} \left(\frac{i\hbar\beta}{2} \right)^4 \frac{d^4}{dt^4} \alpha_{\text{Kubo}}(t) + \mathcal{O}(\hbar^6). \end{aligned} \quad (13)$$

It is interesting that the series Eq. (13) has only a single imaginary term. All terms other than $\frac{i\hbar\beta}{2} \dot{\alpha}_{\text{Kubo}}(t)$ are real. This is only true for the Kubo-transformed correlation function. There has been much work done on relating a classical correlation function to the corresponding quantum correlation function.^{28–30} Such expansions structurally look similar to Eq. (13). However, when the quantum correlation function is expanded in terms of the classical correlation function, there are higher order corrections to the imaginary part as well.²⁸ In addition, the harmonic approach to obtaining the quantum correlation function from the classical correlation function has exactly the same form as here. However, in the harmonic approach, it is an approximation, whereas here it is rigorously true.

If one uses a classical correlation function to approximate $\alpha_{\text{Kubo}}(t)$ and includes only up to the term linear in \hbar in Eq. (13), one would recover the results corresponding to CA. To summarize, Allen *et al.*²² proposed that the real part of the η -coefficients be obtained by doing a quadrature,

$$\text{Re } \eta_{kk'}^{(0)} = \int_{(k-\frac{1}{2})\Delta t}^{(k+\frac{1}{2})\Delta t} dt' \int_{(k'-\frac{1}{2})\Delta t}^{(k'+\frac{1}{2})\Delta t} dt'' \alpha_{\text{Kubo}}(t' - t''), \quad (14)$$

[the superscript (0) is there to indicate that this is the uncorrected version] and for the imaginary part,

$$\text{Im } \eta_{kk'} = \frac{\hbar\beta}{2} \int_{(k-\frac{1}{2})\Delta t}^{(k+\frac{1}{2})\Delta t} dt' \int_{(k'-\frac{1}{2})\Delta t}^{(k'+\frac{1}{2})\Delta t} dt'' \dot{\alpha}_{\text{Kubo}}(t' - t''), \quad (15)$$

they evaluated the “inner” integral analytically, thereby transforming the term into a single integral of the correlation function.

It is easy to see that the first order of correction to the real part of the η -coefficients can be calculated analytically from Eq. (13). On analytically simplifying the expressions for the first order corrections, one finds that it is in form of different linear combinations of the values of the Kubo correlation function $\alpha_{\text{Kubo}}(t)$,

$$\text{Re } \eta_{kk'} = \text{Re } \eta_{kk'}^{(0)} - \frac{\hbar^2 \beta^2}{12} \int_{(k-\frac{1}{2})\Delta t}^{(k+\frac{1}{2})\Delta t} dt' \int_{(k'-\frac{1}{2})\Delta t}^{(k'+\frac{1}{2})\Delta t} dt'' \ddot{\alpha}_{\text{Kubo}}(t' - t'') \quad (16)$$

$$\begin{aligned} &= \text{Re } \eta_{kk'}^{(0)} - \frac{\hbar^2 \beta^2}{12} (\alpha_{\text{Kubo}}((k-k'+1)\Delta t) \\ &- 2\alpha_{\text{Kubo}}((k-k')\Delta t) + \alpha_{\text{Kubo}}((k-k'-1)\Delta t)), \end{aligned} \quad (17)$$

$$\text{Re } \eta_{00} = \text{Re } \eta_{00}^{(0)} - \frac{\hbar^2 \beta^2}{12} \left(\alpha_{\text{Kubo}}\left(\frac{\Delta t}{2}\right) - \alpha_{\text{Kubo}}(0) \right), \quad (18)$$

$$\text{Re } \eta_{kk} = \text{Re } \eta_{kk}^{(0)} - \frac{\hbar^2 \beta^2}{12} (\alpha_{\text{Kubo}}(\Delta t) - \alpha_{\text{Kubo}}(0)), \quad (19)$$

$$\begin{aligned} \text{Re } \eta_{k0} = \text{Re } \eta_{k0}^{(0)} & - \frac{\hbar^2 \beta^2}{12} \left(\alpha_{\text{Kubo}}\left(\left(k + \frac{1}{2}\right)\Delta t\right) - \alpha_{\text{Kubo}}(k\Delta t) \right. \\ & \left. + \alpha_{\text{Kubo}}((k-1)\Delta t) - \alpha_{\text{Kubo}}\left(\left(k - \frac{1}{2}\right)\Delta t\right) \right), \end{aligned} \quad (20)$$

$$\begin{aligned} \text{Re } \eta_{N0} = \text{Re } \eta_{N0}^{(0)} & - \frac{\hbar^2 \beta^2}{12} (\alpha_{\text{Kubo}}(N\Delta t) - 2\alpha_{\text{Kubo}} \\ & \times \left(\left(N - \frac{1}{2}\right)\Delta t \right) + \alpha_{\text{Kubo}}((N-1)\Delta t)). \end{aligned} \quad (21)$$

Equations (17)–(21) define the current method that we would refer to as the first-order truncated Kubo (TK1) approximation to the eta coefficients. Although the higher order terms in the series require the calculation of the numerical derivatives, it might be possible to estimate them using different correlation functions. This is derived explicitly for the second-order correction term in the [Appendix](#). This second-order truncated Kubo approximation would be referred to as TK2.

The structure of several approaches to approximating the quantum correlation function in terms of the classical^{28,30} is similar to the equations listed above. The first correction term is indeed proportional to the second derivative of the correlation function. The difference is only in the exact prefactor used, all of which are of the form $\frac{\hbar^2 \beta^2}{c}$. (Apart from $c = 12$ derived here, $c = 8$ also appears in certain approximations.) Therefore, the correction terms would also look very similar.

While TK2 can be calculated if required, TK1 is by far the simpler of the two algorithms. It needs no extra information other than the bath response function. Let us, therefore, analyze the TK1 approximation and see if we can use heuristics to improve it. To motivate the changes, consider the behavior of the η -coefficients as estimated by TK1 on lowering the temperature. First, note that the true quantum correlation function would become invariant to a temperature below a certain value. This is because as the temperature is lowered, the thermal density matrix would asymptotically become the same as the density matrix corresponding to the ground state. Consequently, the quantum correlation function would asymptotically tend to the ground state correlation function. However, this is not the case with the truncated Kubo approximations.

The uncorrected real part, $\text{Re } \eta^{(0)}$, would show a behavior identical to the Kubo correlation function. To understand the dependence on β , consider the Kubo-transformed position autocorrelation function of a harmonic oscillator,

$$C_{\text{Kubo}}^{xx}(t) = \frac{1}{\beta m \omega^2} \cos(\omega t). \quad (22)$$

Clearly, the correlation function goes to zero as β^{-1} . Consequently, $\text{Re } \eta^{(0)}$ would also go to zero as β^{-1} . The correction term has a prefactor β^2 and, hence, overall would increase linearly with β . This means that the corrected $\text{Re } \eta$ terms would overall increase as β . [This problem arises because we are truncating the infinite series in Eq. (13) after the quadratic term in \hbar . In fact, the second-order term incorporated in TK2 is a worse offender. It would grow as β^3 as $\beta \rightarrow \infty$. We will demonstrate in Sec. III that though TK2 increases the range of temperature where we can get good η -coefficients, its errors increase extremely fast once out of this “good region.”] The imaginary part is independent of β because of its prefactor.

While to correct this issue, we would need to consider the infinite series, here, we give a poor man’s *ad hoc* approximate way of treating the symptom. The uncorrected real part $\text{Re } \eta^{(0)}$ is closely related to the classical correlation function, so we do not change it. Now, turning to the first order correction term, the current coefficient is $-\frac{1}{3} \left(\frac{\hbar \beta}{2} \right)^2$. To get rough temperature independence at very low temperatures, we need to have the prefactor grow linearly with β as that would compensate the β^{-1} scaling of the correlation function. However, this new term has to be equal to the current coefficient and grow as β^2 for $\beta \rightarrow 0$. The function $x \tanh(x)$ has this property of behaving like x^2 for small values of x and as x for large values of x . Therefore, we utilize this intuition to come up with two related but slightly different schemes for regularization (the difference being in how the prefactor is split up):

1. Use $-\frac{1}{3} \left(\frac{\hbar^2 \beta}{2E_h} \right) \tanh\left(\frac{E_h \beta}{2}\right)$ as the prefactor. This is called the tanh1 approximation. This particular grouping of terms can be motivated if $x = \frac{\beta}{2}$ is seen as the main variable. Although β is the term that diverges, it is always seen to appear in the form of $\frac{\hbar \beta}{2}$.
2. Use $-\frac{1}{3} \left(\frac{\hbar^2 \beta}{4E_h} \right) \tanh(E_h \beta)$ as the prefactor. This is called the tanh2 approximation. Here, $x = \beta$ is considered to be the variable. This is extremely natural considering that β is the variable that diverges and we are regularizing for.

(The Hartree energy terms are incorporated to make the argument of the hyperbolic tangent function dimensionless. All the simulations here are done in atomic units and consequently $\hbar = 1$ and $E_h = 1$.) The logic behind differentiating between these two different techniques for taking care of the low temperature behavior is that in the first case, $\frac{\beta}{2}$ is taken as a unit because it came from $\frac{\omega \beta}{2}$ in the reciprocal space. In the second case, we do not keep the entire numerical multiplier outside the hyperbolic tangent. These are both correct at high temperatures but would have different ranges of validity at low temperatures. Furthermore, though not done here, the same idea can quite simply be extended to correct TK2 as well.

III. RESULTS

Consider the family of sub-Ohmic, super-Ohmic, and Ohmic spectral densities with exponential cutoffs, given generally as

$$J(\omega) = \frac{\pi}{2} \hbar \xi \frac{\omega^s}{\omega_c^{s-1}} \exp\left(-\frac{\omega}{\omega_c}\right). \quad (23)$$

Because we have the spectral density, this model gives us a good testing ground for exploring the accuracy of the various approximate approaches to calculating the η -coefficients under a variety of situations. Here, we are using the classical correlation function as an approximation to the Kubo-transformed correlation function. The classical correlation function can be obtained analytically as the following integral:

$$\alpha_{\text{Kubo}}(t) = \frac{1}{\pi} \int_0^\infty d\omega \frac{2}{\hbar\omega\beta} J(\omega) \cos(\omega t) \quad (24)$$

$$= \frac{\xi}{\beta} \frac{\cos(s \tan^{-1}(\omega_c t))}{\sqrt{(1 + \omega_c^2 t^2)^s}} \Gamma(s) \omega_c. \quad (25)$$

For the Ohmic bath ($s = 1$), the classical correlation function, Eq. (25), reduces to the well-known Lorentzian form,

$$\alpha_{\text{Kubo}}(t) = \frac{\xi \omega_c}{\beta(1 + \omega_c^2 t^2)}. \quad (26)$$

As a first comparison, let us consider high temperature parameters where the CA method would work the best. Following the original work,²² we use an Ohmic bath with $\hbar\omega_c\beta = 0.15$, $\xi = 1$, and $\Delta t = 1.25\hbar\beta$. We compare some representative values of $\text{Re } \eta_{kk'}$. The imaginary values are not reported because they are the same for all

three methods. Therefore, the errors would be identical. The comparison is given in Table I. While CA performs quite well, the results obtained by the truncated Kubo and the tanh methods are practically exact. There are no differences in the five places of decimal reported in the table. The TK2 approach of course eliminates all error, reducing the relative error to around $10^{-5}\%$, while the other methods have a larger but still completely negligible error of around $10^{-3}\%$.

Keeping all the other parameters the same, let us change the Ohmic bath to a super-Ohmic bath with $s = 2$. The errors are shown in Table II. Unlike the Ohmic case, the errors in $\text{Re } \eta_{kk'}$ when using CA are quite significantly larger. The family of baths given by Eq. (23) reaches a maximum at $\omega = s\omega_c$. Therefore, for a super-Ohmic spectral density, the maximum occurs at a higher frequency, which is at a colder equivalent temperature making CA worse. The errors of the truncated Kubo (TK) and the tanh methods also grow, though they continue to remain less than a hundredth of a percent, and possibly negligible from the standpoint of a dynamics simulation. Unsurprisingly, TK2 performs the best here as well.

It is interesting to study the growth of the error in each of these methods with increasing inverse temperature. Comparisons for the diagonal $\text{Re } \eta_{kk}$ terms and the terms connecting neighboring points $\text{Re } \eta_{k,(k-1)}$ are shown in Fig. 1. The range of temperature

TABLE I. Comparison of the methods for $s = 1$, $\hbar\omega_c\beta = 0.15$, $\xi = 1$, and $\Delta t = 1.25\hbar\beta$. Parameters are taken from Ref. 22. Only the magnitudes of the relative percentage errors are reported. For this parameter, there is practically no difference between the truncated Kubo and the tanh approaches, and both are practically exact. Where the differences are slightly more prominent (e.g., the first three rows), the tanh correction seems to improve the results.

	From $J(\omega)$	CA	CA, Δ (%)	TK1	TK1, Δ (%)	TK2	TK2, Δ (%)	tanh	tanh Δ (%)	tanh2	tanh2 Δ (%)
$\text{Re } \eta_{00}$	0.029 32	0.029 21	0.369 28	0.029 32	0.001 62	0.029 32	0.000 03	0.029 32	0.000 93	0.029 32	0.001 13
$\text{Re } \eta_{10}$	0.114 74	0.114 36	0.332 02	0.114 74	0.001 19	0.114 74	0.000 01	0.114 74	0.000 57	0.114 74	0.001 28
$\text{Re } \eta_{11}$	0.116 75	0.116 33	0.361 54	0.116 75	0.001 53	0.116 75	0.000 02	0.116 75	0.000 85	0.116 75	0.001 17
$\text{Re } \eta_{20}$	0.105 65	0.105 43	0.207 12	0.105 65	0.000 03	0.105 65	0.000 01	0.105 65	0.000 36	0.105 65	0.001 51
$\text{Re } \eta_{21}$	0.225 66	0.224 97	0.305 38	0.225 66	0.000 92	0.225 66	0.000 01	0.225 66	0.000 35	0.225 66	0.001 36
$\text{Re } \eta_{30}$	0.092 46	0.092 41	0.052 57	0.092 46	0.000 79	0.092 46	0.000 01	0.092 46	0.000 89	0.092 46	0.001 18
$\text{Re } \eta_{31}$	0.205 00	0.204 65	0.169 38	0.205 00	0.000 21	0.205 00	0.000 01	0.205 00	0.000 53	0.205 00	0.001 47
$\text{Re } \eta_{20,1}$	0.017 12	0.017 14	0.074 52	0.017 12	0.000 03	0.017 12	0.000 00	0.017 12	0.000 17	0.017 12	0.000 59
$\text{Re } \eta_{30,1}$	0.007 67	0.007 67	0.035 31	0.007 67	0.000 01	0.007 67	0.000 00	0.007 67	0.000 07	0.007 67	0.000 27

TABLE II. Comparison of the methods for a super-Ohmic bath with $s = 2$. The rest of the parameters are identical to Table I. Even in the worst case scenario, the corrected methods (TK and the tanh correction) are two orders of magnitude better.

	From $J(\omega)$	CA	CA, Δ (%)	TK1	TK1, Δ (%)	TK2	TK2, Δ (%)	tanh	tanh Δ (%)	tanh2	tanh2 Δ (%)
$\text{Re } \eta_{00}$	0.029 44	0.029 12	1.093 47	0.029 45	0.007 96	0.029 44	0.000 17	0.029 45	0.005 90	0.029 44	0.000 23
$\text{Re } \eta_{10}$	0.110 29	0.109 26	0.940 97	0.110 30	0.005 30	0.110 29	0.000 08	0.110 30	0.003 53	0.110 29	0.001 73
$\text{Re } \eta_{11}$	0.116 23	0.114 99	1.061 96	0.116 24	0.007 38	0.116 23	0.000 15	0.116 23	0.005 38	0.116 23	0.000 57
$\text{Re } \eta_{20}$	0.085 15	0.084 82	0.391 50	0.085 15	0.002 19	0.085 15	0.000 12	0.085 15	0.002 92	0.085 15	0.005 08
$\text{Re } \eta_{21}$	0.209 69	0.207 94	0.831 96	0.209 70	0.003 63	0.209 69	0.000 03	0.209 69	0.002 07	0.209 68	0.002 58
$\text{Re } \eta_{30}$	0.053 68	0.053 92	0.449 52	0.053 68	0.008 14	0.053 68	0.000 13	0.053 68	0.007 29	0.053 68	0.004 74
$\text{Re } \eta_{31}$	0.154 54	0.154 20	0.216 49	0.154 53	0.003 76	0.154 54	0.000 13	0.154 53	0.004 16	0.154 53	0.005 34
$\text{Re } \eta_{20,1}$	-0.014 62	-0.014 62	0.044 07	-0.014 62	0.000 00	-0.014 62	0.000 00	-0.014 62	0.000 08	-0.014 62	0.000 32
$\text{Re } \eta_{30,1}$	-0.007 17	-0.007 17	0.029 48	-0.007 17	0.000 00	-0.007 17	0.000 00	-0.007 17	0.000 06	-0.007 17	0.000 22

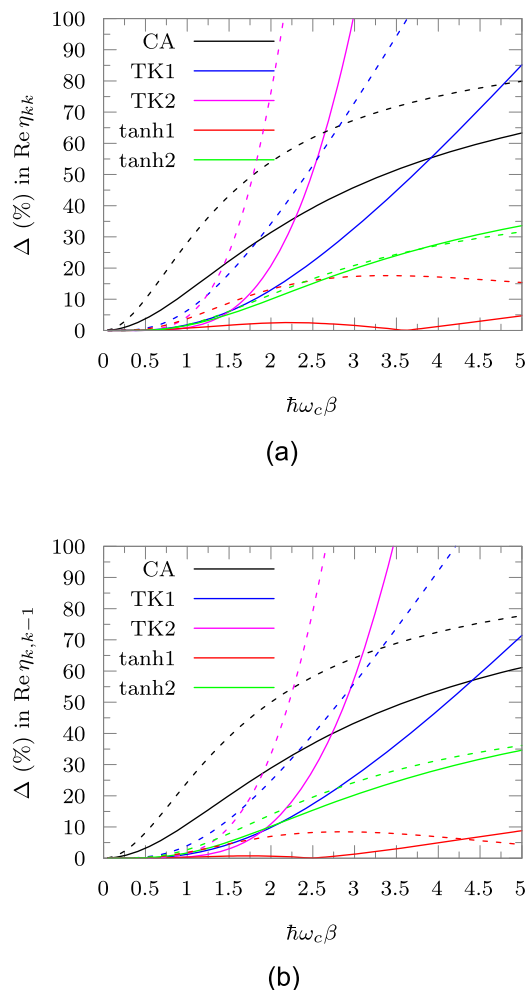


FIG. 1. Percentage error in various discretized influence functional coefficients for each of the methods. Solid lines: Ohmic spectral density. Dashed lines: super-Ohmic spectral density ($s = 2$). The plot goes to very cold temperatures as an illustration of the principle. The errors make the methods useless much earlier. (a) Percentage error in the real part of the diagonal η -coefficients. (b) Percentage error in the real part of the “nearest neighbor interactions,” $\eta_{k,k-1}$.

illustrated in the figure is of course far beyond what any of the three methods can handle. This is just a demonstration of how the errors grow and not a statement about the usability of any of the methods. We can clearly see that both of the corrected methods perform significantly better than the original CA, increasing the region of applicability substantially. Using a 10% relative error as a threshold of applicability, we note that CA becomes inaccurate at $\hbar\omega_c\beta = 1$. This is in comparison to the corrected methods that extend the accuracy at least to $\hbar\omega_c\beta = 2$. Also, it is extremely gratifying that our tanh correction hacks perform exceptionally well and, consistently, better than the base truncated Kubo method. In fact, because of the discrepancy in the scaling of both TK1 and TK2 with β , we find that though they do increase the range of applicability, beyond

that the error increases extremely fast. The fact that TK2 scales as β^3 while TK1 scales as β for $\beta \rightarrow \infty$ gets reflected in the fact that TK1 becomes more accurate beyond around $\hbar\omega_c\beta \approx 1.75$. Now, it is debatable whether any of the TK methods should be used beyond that inverse temperature any way.

While it is illuminating to explore the errors in certain η -coefficients, it is at the end of the day not all that useful. The main problem is that it is difficult to extrapolate errors in the η -coefficients to the error in the dynamical observables one may be interested in. The discrepancies in certain η -coefficients may not reflect as much and others may reflect more because of the way different path amplitudes interact. The only real way of judging this is by simulating the dynamics of a two-level system coupled to the bath by using different methods for calculating the influence functional coefficients. The simulations of dynamics that follow have been done using the iterative quasi-adiabatic propagator path integral (QuAPI)¹⁰ method.

For the examples with dynamics, we will consider a more difficult case for these high temperature methods. The system is symmetric and defined by $\hat{H}_0 = -\hbar\Omega\hat{\sigma}_x$. Consider an Ohmic bath with $\xi = 1.5$, $\omega_c = 2.5\Omega$. The faster bath means that the effective temperature would be lower. We start with a high temperature of $\hbar\omega_c\beta = 0.25$. (The simulations were converged at a time-step of $\Omega\Delta t = 0.125$ and a non-Markovian memory length of $L\Omega\Delta t = 1.25$.) This is the regime where all the methods should be equivalently good. The dynamics of $\hat{\sigma}_z$ and $\hat{\sigma}_x$ are shown in Fig. 2. While the dynamics of $\hat{\sigma}_z$ is identical in all the methods, we can, even at this high temperature, visibly see the error in the CA simulation of $\hat{\sigma}_x(t)$. Both the truncated Kubo and the tanh corrections agree exactly with the result from the analytic η -coefficients. Therefore, this error cannot be a result of any error in $\text{Im } \eta_{kk}$ because that is common to all three methods. Lowering the temperature to $\hbar\omega_c\beta = 2$, in Fig. 3, one finds that the CA method has fallen apart. Both TK and the tanh corrections continue to give acceptable results for $\hat{\sigma}_z(t)$ but the TK1 and TK2 results for $\hat{\sigma}_x(t)$ do not match the analytical results. While the tanh1 approach seems to be quite close to the TK1 method, tanh2 continues to give extremely good agreement with the fully analytical result.

In fact, even at $\hbar\omega_c\beta = 4$, the tanh2 correction gives quite acceptable results. This is shown in Fig. 4. At this very low temperature, we see the effects of the extreme sharp rise of errors in the TK2 method. We had mentioned that though TK2 increases the range of applicability of the method, at low temperatures, the scaling of TK2 (β^3) is very different from the theoretical limits, where the correlation function should be independent of β . Here, we see such a very low temperature, where the TK2 approach is in fact even worse than CA.

Thus, we see that all the methods discussed here significantly increase the range of applicability of the correlation function-based approach to calculating the discretized influence functional coefficients. Through rigorous derivations of TK1 and TK2, we have increased the range of temperatures by at least two-fold. Although the two tanh corrections have slightly different prefactors, they both perform quite well with the tanh2 correction being the best. It is pleasantly surprising that with tanh2, we have attained an almost fourfold increase in the temperature range over which we can get accurate dynamics.

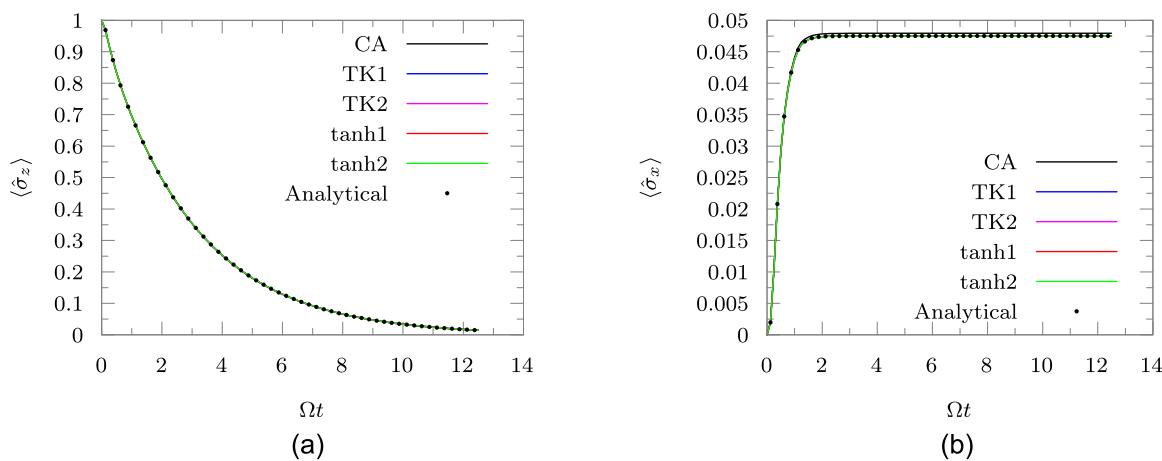


FIG. 2. Dynamics of various operators using different methods of generating the η -coefficients at a temperature of $\hbar\omega_c\beta = 0.25$. (a) Dynamics of the $\sigma_z(t)$. (b) Dynamics of the $\sigma_x(t)$.

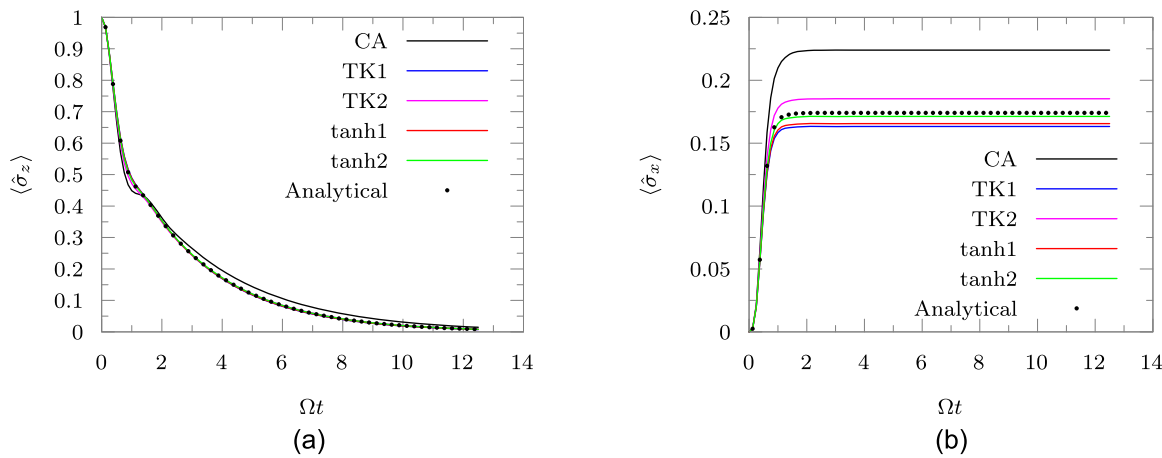


FIG. 3. Dynamics of various operators using different methods of generating the η -coefficients at a temperature of $\hbar\omega_c\beta = 2$. (a) Dynamics of the $\sigma_z(t)$. (b) Dynamics of the $\sigma_x(t)$.

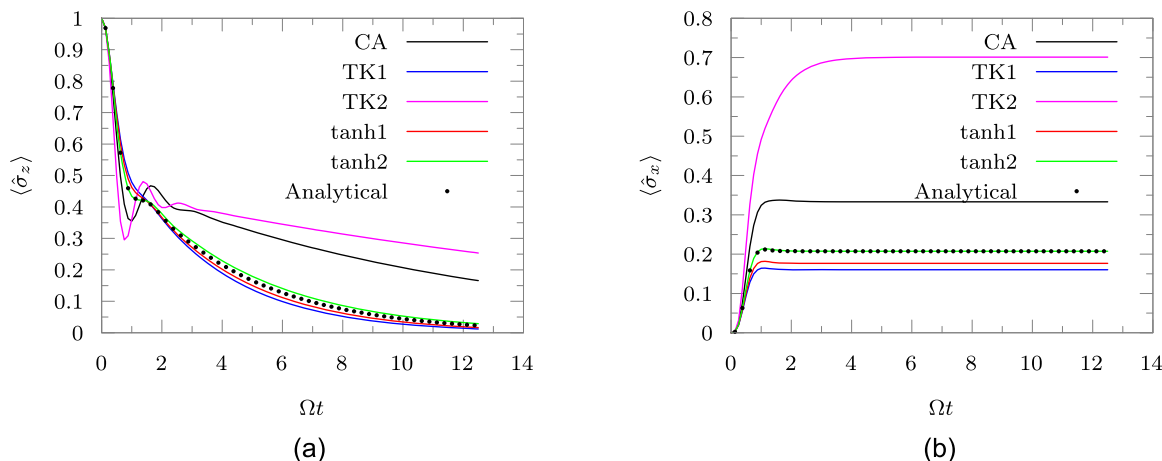


FIG. 4. Dynamics of various operators using different methods of generating the η -coefficients at a temperature of $\hbar\omega_c\beta = 4$. (a) Dynamics of the $\sigma_z(t)$. (b) Dynamics of the $\sigma_x(t)$.

IV. CONCLUSION

We have developed a systematic way of expressing the η -coefficients in terms of the Kubo-transformed bath response function. This makes it possible to use the results from methods such as RPMD and CMD to characterize the mapping of an *ab initio* atomistic solvent onto a bath of harmonic oscillators. The Kubo-transformed correlation function, though identical in information content to the standard quantum correlation function, is more classical in the symmetries that it has. Therefore, if a classical correlation function is used as an approximation to the Kubo-transformed correlation function and this expression is truncated at the first order in \hbar , it reduces to the classical approximation.²² While the classical approximation was an *ad hoc* approach, the relationship derived over here can be used to rigorously converge the values of the η -coefficients.

In addition to the general series, we have presented a host of useful and cheap corrections to the classical approximation, thereby increasing the temperature range over which one can directly compute the discretized influence functional coefficients from correlation functions. We have shown how the first major correction to the classical approximation scheme can be analytically integrated leading to a very simple change to the exact expressions. This change can be obtained for no extra computational cost over the integrals required to get the classical approximation. This first change is called the first-order truncated Kubo expression. Although further terms can, in principle, be incorporated, they require the calculation of numerical derivatives or separate costly correlation functions. If the original data are noisy, such computations are often numerically unstable. Thus, it is tempting to stop at this first order. Interestingly, for the case of the second-order correction, we have derived a relationship of this term with a different correlation function that can also be estimated quite efficiently by molecular dynamics.

Because TK2 requires the calculation of an extra correlation function, it is not always very lucrative. It is interesting to think about improving TK1 with some heuristics. We have analyzed the behavior of TK1 and shown that the real part scales linearly with the inverse temperature, β . This is a problem because, at very low temperatures, the correlation function should asymptotically tend to the ground state correlation function. The cause was seen to be the truncation of the infinite series. However, we have proposed a “poor-man’s” approximation that involves transforming the coefficient of the correction term to respect the proper limits. This constitutes the motivation behind the two tanh approximations that have been derived.

We have numerically assessed the performance of various approximations introduced here to the classical approximation and the analytical η -coefficients obtained using the expressions in Ref. 10. (These numerical explorations have been done on a harmonic bath, where the classical and Kubo correlation functions are the same. For calculations on anharmonic solvents, ideally, an approximate Kubo correlation function like the one from RPMD or CMD should be used. In the absence of such an approximation, the classical correlation function can also be used because of the similarities that the Kubo function shares with it.) We showed that the exact values of the η -coefficients calculated by the TK and the tanh approaches, even at high temperatures, are significantly

closer to the analytical results compared to the CA method. The newly introduced corrections yield more accurate η -coefficients through the entire applicable range of temperature. Despite this overall increase in accuracy, it is noted that TK2 breaks down quite pathologically. This has been understood from the perspective of scaling with the inverse temperature, β , which can only be truly solved by considering the entire infinite series or, equivalently, working in the frequency domain. While the true bath response function becomes independent of β at very low temperatures, the TK approximations do not. In fact, the TK2 approach grows as β^3 . This is what leads to the pathological breakdown. Because the various tanh approximations were built to fix this problem heuristically, it is very encouraging that they perform significantly better than TK approaches at low temperatures.

The values of these discretized influence functional coefficients, while extremely crucial, interact with the path amplitude and the path sum in non-trivial ways making an extrapolation of errors in coefficients to errors in dynamics impossible. We simulated the dynamics of a two-level system coupled to an Ohmic bath at different temperatures with coefficients being derived by each of the four approximate correlation function-based approaches. The corrections introduced here increase the temperature range of applicability of the correlation function-based approach by almost four times in the best case. While the numerical results shown here pertain to model spectral densities, real biological or chemical systems cannot be described only using the unstructured low frequency modes. They have a mixture of a broad low frequency spectrum and sharp features, mostly at higher frequencies, arising from more rigid molecular vibrations. The corrections for low temperatures would be even more important there. The rigid vibration regions are typically colder than the unstructured ro-translational region of the spectral density. Of course, if the simulation is done at a cold enough temperature and all the higher order terms are necessary, it would possibly be the simplest to calculate the spectral density directly because of problems with the numerical derivatives and the scaling with β .

The incorporation of Kubo correlation functions in path integral-based approaches to system-solvent quantum dynamics seems a very lucrative way of including anharmonic nuclear quantum effects in the solvent in a simple way. Here, we have just scratched the surface of this deep relationship. Future work would look into further connections and possibilities.

ACKNOWLEDGMENTS

I acknowledge support of the Computational Chemical Science Center: Chemistry in Solution and at Interfaces funded by the U.S. Department of Energy (Award No. DE-SC0019394).

AUTHOR DECLARATIONS

Conflict of Interest

The authors have no conflicts to disclose.

Author Contributions

Amartya Bose: Conceptualization (equal); Data curation (equal); Formal analysis (equal); Funding acquisition (equal); Investigation

(equal); Methodology (equal); Resources (equal); Software (equal); Validation (equal); Visualization (equal); Writing – original draft (equal); Writing – review & editing (equal).

DATA AVAILABILITY

The data that support the findings of this study are available from the corresponding author upon reasonable request.

APPENDIX: RELATION BETWEEN THE SECOND-ORDER CORRECTION AND CLASSICAL CORRELATION FUNCTION

In the body of the text, we have focused on the first-order correction to CA, primarily because that is the most important term and can be evaluated at zero additional cost. While the higher order corrections can be generally obtained using appropriate numerical derivatives, it is possible to obtain the second-order correction quite efficiently using a different set of correlation functions.

Consider the second-order correction term to the bath response function, Eq. (13), given as $-\frac{\hbar^4 \beta^4}{720} \frac{d^4}{dt^4} \alpha_{\text{Kubo}}(t)$. The corresponding correction to the discretized influence functional coefficients would be given as a double integral of the same,

$$\varepsilon_{kk'} = -\frac{\hbar^4 \beta^4}{720} \int_{(k-\frac{1}{2})\Delta t}^{(k+\frac{1}{2})\Delta t} dt' \int_{(k'-\frac{1}{2})\Delta t}^{(k'+\frac{1}{2})\Delta t} dt'' \alpha_{\text{Kubo}}^{(iv)}(t' - t''). \quad (\text{A1})$$

By analytically doing the integrals, we can express the correction as

$$\varepsilon_{kk'} = -\frac{\hbar^4 \beta^4}{720} \left(\ddot{\alpha}_{\text{Kubo}}((k-k'+1)\Delta t) - 2\ddot{\alpha}_{\text{Kubo}}((k-k')\Delta t) + \ddot{\alpha}_{\text{Kubo}}((k-k'-1)\Delta t) \right). \quad (\text{A2})$$

Therefore, the second-order correction term to CA requires second-order derivatives of the correlation function.

For simplicity, let us assume that the classical correlation function is used instead of the Kubo-transformed correlation function. Therefore, we replace α_{Kubo} with α_{Cl} . Since RPMD and CMD both are classical trajectory-based methods for approximating the correlation function, a similar derivation can also be done for the relevant expressions corresponding to the two approximately quantum methods. The bath response function in its quantum form and its classical approximation are given as

$$\alpha(t) \propto \langle \hat{f}(t)\hat{f}(0) \rangle, \quad (\text{A3})$$

$$\alpha_{\text{Cl}}(t) \propto \iint d\mathbf{q}_0 d\mathbf{p}_0 e^{-\beta H(\mathbf{q}_0, \mathbf{p}_0)} f(\mathbf{q}_0) f(\mathbf{q}_t). \quad (\text{A4})$$

The first derivative of $\alpha_{\text{Cl}}(t)$ can be expressed as

$$\dot{\alpha}_{\text{Cl}}(t) \propto \iint d\mathbf{q}_0 d\mathbf{p}_0 e^{-\beta H(\mathbf{q}_0, \mathbf{p}_0)} f(\mathbf{q}_0) \left(\vec{f}'(\mathbf{q}_t) \cdot \frac{\mathbf{p}_t}{m} \right), \quad (\text{A5})$$

where \vec{f}' is the gradient of the function f . The second temporal derivative can be expressed by the chain-rule,

$$\ddot{\alpha}_{\text{Cl}}(t) \propto \iint d\mathbf{q}_0 d\mathbf{p}_0 e^{-\beta H(\mathbf{q}_0, \mathbf{p}_0)} f(\mathbf{q}_0) \times \left(\frac{\mathbf{p}_t^T}{m} \cdot \overline{\overline{f''}}(\mathbf{q}_t) \cdot \frac{\mathbf{p}_t}{m} - \vec{f}'(\mathbf{q}_t) \cdot \frac{\mathbf{F}(\mathbf{q}_t)}{m} \right). \quad (\text{A6})$$

The second-order derivative of f with respect to the position is denoted by $\overline{\overline{f''}}(\mathbf{q}_t)$. Generally, storing such second-order derivatives is challenging, but, here, one can calculate them on-the-fly and directly calculate the dot products. The force on the particle is given by \mathbf{F} .

Thus, it is possible to express the second-order time derivative of the autocorrelation function in terms of cross-correlation functions, Eq. (A6). Consequently, if required, one can evaluate the correction term, Eq. (A2), in terms of this cross-correlation function.

REFERENCES

- ¹J. H. Van Vleck, "The correspondence principle in the statistical interpretation of quantum mechanics," *Proc. Natl. Acad. Sci. U. S. A.* **14**, 178 (1928).
- ²M. F. Herman and E. Kluk, "A semiclassical justification for the use of non-spreading wavepackets in dynamics calculations," *Chem. Phys.* **91**, 27 (1984).
- ³W. H. Miller, "An alternate derivation of the Herman-Kluk (coherent state) semiclassical initial value representation of the time evolution operator," *Mol. Phys.* **100**, 397 (2002).
- ⁴E. P. Wigner, "Some remarks on the theory of reaction rates," *J. Chem. Phys.* **7**, 646 (1939).
- ⁵E. Wigner, "On the quantum correction for thermodynamic equilibrium," *Phys. Rev.* **40**, 749 (1932).
- ⁶J. Cao and G. A. Voth, "The formulation of quantum statistical mechanics based on the Feynman path centroid density. I. Equilibrium properties," *J. Chem. Phys.* **100**, 5093 (1994).
- ⁷J. Cao and G. A. Voth, "The formulation of quantum statistical mechanics based on the Feynman path centroid density. II. Dynamical properties," *J. Chem. Phys.* **100**, 5106 (1994).
- ⁸I. R. Craig and D. E. Manolopoulos, "Quantum statistics and classical mechanics: Real time correlation functions from ring polymer molecular dynamics," *J. Chem. Phys.* **121**, 3368 (2004).
- ⁹Y. Tanimura and R. Kubo, "Time evolution of a quantum system in contact with a nearly Gaussian-Markoffian noise bath," *J. Phys. Soc. Jpn.* **58**, 101 (1989).
- ¹⁰N. Makri and D. E. Makarov, "Tensor propagator for iterative quantum time evolution of reduced density matrices. I. Theory," *J. Chem. Phys.* **102**, 4600 (1995).
- ¹¹N. Makri and D. E. Makarov, "Tensor propagator for iterative quantum time evolution of reduced density matrices. II. Numerical methodology," *J. Chem. Phys.* **102**, 4611 (1995).
- ¹²Q. Shi, Y. Xu, Y. Yan, and M. Xu, "Efficient propagation of the hierarchical equations of motion using the matrix product state method," *J. Chem. Phys.* **148**, 174102 (2018).
- ¹³Y. Yan, T. Xing, and Q. Shi, "A new method to improve the numerical stability of the hierarchical equations of motion for discrete harmonic oscillator modes," *J. Chem. Phys.* **153**, 204109 (2020).
- ¹⁴Y. Yan, M. Xu, T. Li, and Q. Shi, "Efficient propagation of the hierarchical equations of motion using the Tucker and hierarchical Tucker tensors," *J. Chem. Phys.* **154**, 194104 (2021).
- ¹⁵A. Strathearn, P. Kirton, D. Kilda, J. Keeling, and B. W. Lovett, "Efficient non-Markovian quantum dynamics using time-evolving matrix product operators," *Nat. Commun.* **9**, 3322 (2018).

- ¹⁶A. Bose and P. L. Walters, "A tensor network representation of path integrals: Implementation and analysis," [arxiv:2106.12523](https://arxiv.org/abs/2106.12523) (2021).
- ¹⁷A. Bose, "Pairwise connected tensor network representation of path integrals," *Phys. Rev. B* **105**, 024309 (2022).
- ¹⁸R. P. Feynman and F. L. Vernon, "The theory of a general quantum system interacting with a linear dissipative system," *Ann. Phys.* **24**, 118 (1963).
- ¹⁹A. Bose and P. L. Walters, "A multisite decomposition of the tensor network path integrals," *J. Chem. Phys.* **156**, 024101 (2022).
- ²⁰A. Bose and P. L. Walters, "Tensor network path integral study of dynamics in B850 LH2 ring with atomistically derived vibrations," *J. Chem. Theory Comput.* **18**(7), 4095–4108 (2022).
- ²¹A. Bose, "Effect of phonons and impurities on the quantum transport in XXZ spin-chains" [arXiv:2206.11156](https://arxiv.org/abs/2206.11156) (2022).
- ²²T. C. Allen, P. L. Walters, and N. Makri, "Direct computation of influence functional coefficients from numerical correlation functions," *J. Chem. Theory Comput.* **12**, 4169 (2016).
- ²³L. Zhang, M. Chen, X. Wu, H. Wang, W. E, and R. Car, "Deep neural network for the dielectric response of insulators," *Phys. Rev. B* **102**, 041121(R) (2020).
- ²⁴L. Zhang, J. Han, H. Wang, R. Car, and W. E, "Deep potential molecular dynamics: A scalable model with the accuracy of quantum mechanics," *Phys. Rev. Lett.* **120**, 143001 (2018).
- ²⁵K. Vanommeslaeghe, E. Hatcher, C. Acharya, S. Kundu, S. Zhong, J. Shim, E. Darian, O. Guvench, P. Lopes, I. Vorobiov, and A. D. Mackerell, Jr., "CHARMM general force field: A force field for drug-like molecules compatible with the CHARMM all-atom additive biological force fields," *J. Comput. Chem.* **31**, 671 (2010).
- ²⁶R. Lambert and N. Makri, "Quantum-classical path integral. I. Classical memory and weak quantum nonlocality," *J. Chem. Phys.* **137**, 22A552 (2012).
- ²⁷R. Lambert and N. Makri, "Quantum-classical path integral. II. Numerical methodology," *J. Chem. Phys.* **137**, 22A553 (2012).
- ²⁸H. Kim and P. J. Rossky, "Evaluation of quantum correlation functions from classical data," *J. Phys. Chem. B* **106**, 8240 (2002).
- ²⁹H. Kim and P. J. Rossky, "Evaluation of quantum correlation functions from classical data: Anharmonic models," *J. Chem. Phys.* **125**, 074107 (2006).
- ³⁰S. A. Egorov, K. F. Everitt, and J. L. Skinner, "Quantum dynamics and vibrational relaxation," *J. Phys. Chem. A* **103**, 9494 (1999).